



## Effect of fruit extracts of some environmentally benign green corrosion inhibitors on corrosion of mild steel in hydrochloric acid solution

Ambrish Singh<sup>a</sup>, V. K. Singh<sup>a</sup>, M. A. Quraishi<sup>b\*</sup>

<sup>a</sup> Department of Chemistry, Udai Pratap Autonomous College, Varanasi 221002 (India)

<sup>b</sup> Department of Applied Chemistry, Institute of Technology  
Banaras Hindu University, Varanasi 221005 (India)

Received in 29 Oct 2010, Revised 14 Nov 2010, Accepted 18 Nov 2010.

\*Corresponding Author Email: [maquraishi.apc@itbhu.ac.in](mailto:maquraishi.apc@itbhu.ac.in); [maquraishi@rediffmail.com](mailto:maquraishi@rediffmail.com); Ph.no. +91-9307025126;  
Fax: +91- 542- 2368428

### Abstract

The inhibition of the corrosion of mild steel in hydrochloric acid solution by the fruits extract of Shahjan (*Moringa oleifera*), Pipali (*Piper longum*) and Orange (*Citrus aurantium*) has been studied using weight loss, electrochemical impedance spectroscopy, potentiodynamic polarization and linear polarization techniques. Inhibition was found to increase with increasing concentration of the extract. The effect of temperature, immersion time and acid concentration on the corrosion behavior of mild steel in 1 M HCl with addition of extract was also studied. The adsorption of the extract on the mild steel surface obeyed the Langmuir adsorption isotherm. Values of inhibition efficiency calculated from weight loss, potentiodynamic polarization, and electrochemical impedance spectroscopy (EIS) are in good agreement. Polarization curves showed that fruits extract behaves as a mixed-type inhibitor in hydrochloric acid. The activation energy as well as other thermodynamic parameters for the inhibition process was calculated. The adsorbed film on mild steel surface containing fruits extract was also measured by Fourier transform infrared spectroscopy (FTIR). The results obtained showed that the fruits extract could serve as effective inhibitor of the corrosion of mild steel in hydrochloric acid media.

**Keywords:** Corrosion inhibition; Mild steel; electrochemical measurement; FTIR; Hydrochloric acid

### 1. Introduction

Inhibitors are frequently used for controlling corrosion of metals and alloys in acidic media for removing scales and rusts in metal finishing industries, cleaning of boilers and heat exchangers. Use of inhibitors is one of the most practical methods for protection against corrosion especially in acid solutions to prevent unexpected metal dissolution and acid consumption [1, 2]. The known hazardous effect of most synthetic corrosion inhibitors have motivated scientists to use naturally occurring products as corrosion inhibitors as they are inexpensive, readily available and renewable sources of materials, environmentally friendly and ecologically acceptable [3,4].

Up till now saps of certain plant leaves such as *Murraya koenigii*, *Embilica officianilis*, *Terminalia chebula*, *Terminalia belivina*, *Sapindus trifolianus*, *Accacia conicianna*, *Swertia angustifolia*, *Eugenia jambolans*, *Pongamia glabra*, *Annona squamosa*, *Accacia Arabica*, *Occimum viridis*, *Telferia occidentalis*, *Carica papaya*, *Azadirachta indica*, *Vernonia amydalina*, *Nypa fructicans* wurmb, *Ricimus communis* coriander, hibiscus, Eucalyptus, anis, black cumin and garden cress have been studied for the corrosion inhibition of mild steel in acid media [5-11]. Some of the fruits such as Tobacco, castor oil fruits, acacia gum and lignin along with *Papaia*, *Poinciana pulcherrima*, *Cassia occidentalis* and *Datura stramonium* have also been used as efficient corrosion inhibitor for steel [12-16]. The anticorrosion activity of onion, garlic and bitter melon for mild steel in acid media showed good results studied. Oil extracts of Ginger, jojoba, eugenol, acetyl-eugenol, *artemisia* oil and *Mentha pulegium* are used for corrosion

inhibition of steel in acid media [17, 18]. Saps of certain plants is very useful corrosion inhibitors. *Calotropis procera*, *Azydracta indica* and *Auforpio turkiale* sap are useful as acid corrosion inhibitors. Quinine has been studied for its anticorrosive effect of carbon steel in 1 M HCl. The inhibition effect of *Zenthoxylum alatum* extract on the corrosion of mild steel in aqueous Orthophosphonic acid was investigated. [19-21].

In continuation of our work on development of green corrosion inhibitors [22-23], the present study investigates the inhibiting effect of some fruits extract Shahjan (*Moringa oleifera*), Pippali (*Piper longum*) and Orange (*Citrus aurantium*) on the corrosion of mild steel in 1 M HCl solution by weight loss, potentiodynamic polarization and electrochemical impedance spectroscopy (EIS) methods. Meanwhile, the steel surface was examined by Fourier transform infrared (FTIR) spectroscopy.

## 2. Experimental

### 2.1. Preparation of Fruits extract

Shahjan (*Moringa oleifera*), Pippali (*Piper longum*) and Orange (*Citrus aurantium*) fruits were dried and grounded to powder form. Dried (10g) powder was soaked in double distilled water (500 mL) and refluxed for 5 h. The aqueous solution was filtered and concentrated to 100 mL. This extract was used to study the corrosion inhibition properties. Corrosion tests were performed on a mild steel of the following percentage composition (wt.%): Fe 99.30%, C 0.076%, Si 0.026%, Mn 0.192%, P 0.012%, Cr 0.050%, Ni 0.050%, Al 0.023%, and Cu 0.135%, which were abraded successively with fine grade emery papers from 600 to 1200 grade. The specimens were washed thoroughly with double distilled water and finally degreased with acetone and dried at room temperature. The aggressive solution 1 M HCl was prepared by dilution of analytical grade HCl (37%) with double distilled water and all experiments were carried out in unstirred solutions.

### 2.2. Weight loss method

Weight loss measurements were performed on the mild steel samples with a rectangular form of size 2.5 cm × 2.0 cm × 0.025 cm in 1 M HCl solution with and without addition of different concentrations of fruit's extract. Every sample was weighed by an electronic balance, and then placed in the acid solution (100 mL). The duration of the immersion was 3 h at the temperature range from 308 to 338 K. After immersion, the surface of the specimen was cleaned by double distilled water followed rinsing with acetone and the sample was weighed again in order to calculate inhibition efficiency ( $\eta$  %) the corrosion rate ( $C_R$ ). The experiments were performed in triplicate and the average value of the weight loss was noted. For each experiment, a freshly prepared solution was used and the solution temperature was thermostatically controlled at a desired value.

The surface coverage ( $\theta$ ) and inhibition efficiency ( $\eta$  %) were determined by using following equations:

$$\theta = \frac{w_0 - w_i}{w_0} \quad (1)$$

$$\eta\% = \frac{w_0 - w_i}{w_0} \times 100 \quad (2)$$

where,  $w_i$  and  $w_0$  are the weight loss values in presence and absence of inhibitor, respectively.

The corrosion rate ( $C_R$ ) of mild steel was calculated using the relation:

$$C_R \text{ (mm / y)} = \frac{87.6 \times w}{atD} \quad (3)$$

where,  $w$  is corrosion weight loss of mild steel (mg),  $a$  the area of the coupon ( $\text{cm}^2$ ),  $t$  is the exposure time (h) and  $D$  the density of mild steel ( $\text{g cm}^{-3}$ ).

### 2.3. Electrochemical measurements

The electrochemical studies were made using a Gamry three electrode cell assembly at room temperature. The mild steel of 1  $\text{cm}^2$  was the working electrode, platinum electrode was used as an auxiliary electrode, and standard calomel electrode (SCE) was used as reference electrode. The working electrode was abraded with different grades of emery papers, washed with water and degreased with acetone. All electrochemical measurements were carried out using Gamry Potentiostat/Galvanostat (Model G-300) with EIS software Gamry Instruments Inc., USA. Gamry applications include software DC 105 for corrosion and EIS 300 for EIS measurements and Echem Analyst version 5.50 software packages for data fitting. Prior to the electrochemical measurement, a stabilization period of 30 minute was allowed, which was proved to be sufficient to attain a stable value of  $E_{\text{corr}}$ .

The linear polarization study was carried out from cathodic potential of -20 mV versus OCP to an anodic potential of +20 mV versus OCP with a sweep rate 0.125  $\text{mV s}^{-1}$  to determine the polarization resistance ( $R_p$ ). From the measured polarization resistance value, the inhibition efficiency has been calculated using the relationship:

$$\eta\% = \frac{R_p' - R_p^0}{R_p'} \times 100 \quad (4)$$

where,  $R_p^0$  and  $R_p^i$  are the polarization resistance in absence and in presence of inhibitor, respectively.

Tafel curves were obtained by changing the electrode potential automatically from -250 to +250 mV versus corrosion potential ( $E_{corr}$ ) at a sweep rate of 1 mV s<sup>-1</sup>. EIS measurements were carried out in a frequency range from 100 kHz to 10 mHz under potentiodynamic conditions, with amplitude of 10 mV peak-to-peak, using AC signal at  $E_{corr}$ . The linear Tafel segments of anodic and cathodic curves were extrapolated to corrosion potential to obtain corrosion current densities ( $I_{corr}$ ). The inhibition efficiency was evaluated from the measured  $I_{corr}$  values using the relationship:

$$\eta\% = \frac{I_{corr}^0 - I_{corr}^i}{I_{corr}^0} \times 100 \tag{5}$$

where,  $I_{corr}^0$  and  $I_{corr}^i$  are the corrosion current in absence and in presence of inhibitor, respectively. The charge transfer resistance values were obtained from the diameter of the semi circles of the Nyquist plots. The inhibition efficiency of the inhibitor has been found out from the charge transfer resistance values using the following equation:

$$\eta\% = \frac{R_{ct}^0 - R_{ct}^i}{R_{ct}^i} \times 100 \tag{6}$$

where,  $R_{ct}^0$  and  $R_{ct}^i$  are the charge transfer resistance in absence and in presence of inhibitor, respectively. All electrochemical measurements were done in unstirred and non de-aerated solutions.

### 2.4. Fourier transform infrared spectroscopy (FTIR)

FTIR spectra were recorded in a Thermo Nicolet-5700 FTIR spectrophotometer (USA). The mild steel specimens of size 2.5 cm × 2.0 cm × 0.025 cm were prepared as described above. These specimens were immersed for 3 h in 100 mL of 1 M HCl solution containing 400 ppm of inhibitor and were then dried. In order to prevent damage of the protective film or layer of the mild steel surfaces, the FTIR reflectance accessory was applied to study the mild steel surfaces.

## 3. Results and discussion

### 3.1. Weight loss Studies

#### 3.1.1. Effect of Inhibitor concentration

Fig. 1a represents the effect of fruits extract concentration on inhibition efficiency in 1 M HCl. The inhibition efficiency increases and on the other hand corrosion rate decreases with increase in the concentration of all fruits extract upto their optimum level after which a further increase in inhibitor concentration did not cause any significant change in  $\eta\%$  and  $C_R$ . The extract of *Moringa oleifera* showed maximum inhibition efficiency of 98.2 % in HCl at an optimum concentration of 300 ppm. Further increase in extract concentration did not cause any significant change in the performance of the extract. The values of percentage inhibition efficiency ( $\eta\%$ ) and corrosion rate ( $C_R$ ) obtained from weight loss method at different concentrations of fruits extract at 308 K are summarized in Table 1.

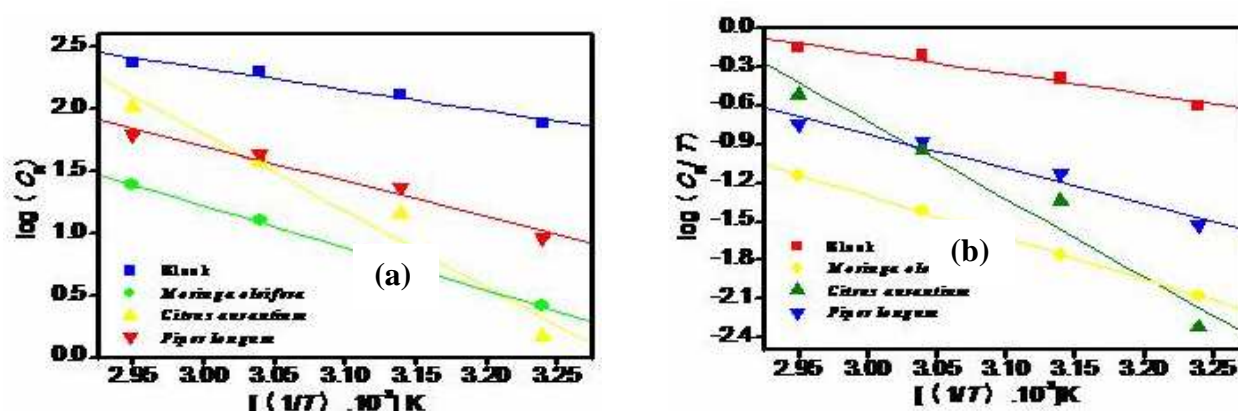


Fig. 2 (a) Arrhenius and (b) Transition state plots

**Table 1** Corrosion parameters for the mild steel in 1 M HCl containing various concentrations of the fruits extract at 308 K obtained from weight loss measurements after 3 h immersion

Inhibitor	Concentration (ppm)	Weight loss (mg cm <sup>-2</sup> )	$\eta$ (%)	$C_R$ (mm y <sup>-1</sup> )
Blank		20.9		77.9
<i>Piper longum</i>	90	7.7	63.3	28.5
	120	7.3	65.2	27.0
	180	2.8	86.6	10.3
	240	2.6	87.6	9.6
	300	1.6	92.3	5.9
	600	0.7	96.6	2.5
<i>Moringa oleifera</i>	50	3.0	85.7	11.1
	100	2.9	86.6	10.7
	150	1.2	94.0	4.4
	200	0.8	96.1	2.9
	250	0.7	96.6	2.5
	300	0.4	98.2	1.4
<i>Citrus aurantium</i>	100	15.6	25.8	57.8
	150	12.5	40.5	46.3
	200	9.3	55.7	34.5
	300	7.0	66.7	25.9
	600	3.2	84.8	11.8
	1200	2.5	88.1	9.2

### 3.1.2. Effect of immersion time

In order to assess the stability of inhibitive behavior of fruit extract on a time scale, weight loss measurements were performed in 1 M HCl in absence and presence of fruits extract for 2 to 8 h immersion time at temperature 308 K. Inhibition efficiencies were plotted against immersion time as seen from Fig. 1b. The inhibition efficiency decreases with increase in immersion time from 2 to 8 h for *Citrus aurantium* and increases for *Moringa oleifera* and *Piper longum*. The value of  $\eta\%$  increased from 25.8% to 88.1% for *Citrus aurantium*, from 85.7 to 98.2% for *Moringa oleifera* and from 63.3 to 96.6% for *Piper longum*. These results suggested that studied fruits extract are effective corrosion inhibitors for mild steel in 1 M HCl solutions.

### 3.1.3. Effect of acid concentration

The variation of inhibition efficiency with increase in acid concentration from 0.5 M to 2 M is shown in Fig. 1c. From this figure it can be seen that inhibition efficiency of fruits extract decreases with increase in HCl concentration from 0.5 M to 2 M. This decrease in efficiency ( $\eta\%$ ) can be attributed to increased aggressiveness of solutions with increase in acid concentration.

### 3.1.4 Effect of temperature

To evaluate the stability of adsorbed layer/film of inhibitor on mild steel surface as well as activation parameters of the corrosion process of steel in acidic medium, weight loss measurements were carried out in the range of temperature 308-338 K in the absence and presence of fruits extract at optimum concentration during 3 h immersion time. Results thus obtained are shown in Fig.1d. It is evident from this Fig. 1d that inhibition efficiency decreases with increasing temperature. This is due to increased rate of dissolution process of mild steel and partial desorption of the inhibitor from the metal surface with temperature [24].

The log of corrosion rate is a linear function of temperature (Arrhenius equation) [25-27]:

$$\log(C_R) = \frac{-E_a}{2.303RT} + A \quad (7)$$

where,  $E_a$  is the apparent effective activation energy,  $R$  is the molar gas constant and  $A$  is Arrhenius pre exponential factor. A plot of log of corrosion rate obtained by weight loss measurement versus  $1/T$  gave a straight line as shown in Fig. 2a with a slope of  $-E_a/2.303R$ . The values of activation energy are listed in Table 2. The data shows that the activation energy ( $E_a$ ) of the corrosion in mild steel in 1 M HCl solution in the presence of fruits extract is higher than that in the free acid solution. The increase in the apparent activation energy for mild steel dissolution in inhibited solution may be interpreted as physical adsorption that occurs in the first stage [28]. Szauer and Brand explained [29] that the increase in activation energy can be attributed to an appreciable decrease in the adsorption of the inhibitor on the mild steel surface with increase in temperature.

An alternative formulation of Arrhenius equation is [30]:

$$C_R = \frac{RT}{Nh} \exp\left(\frac{\Delta S^*}{R}\right) \exp\left(\frac{-\Delta H^*}{RT}\right) \quad (8)$$

where, h is Planck's constant, N is Avogadro's number,  $\Delta S^*$  the entropy of activation, and  $\Delta H^*$  the enthalpy of activation. A plot of  $\log C_R/T$  versus  $1/T$  gave a straight line (fig. 2b) with a slope equal to  $-\Delta H^*/2.303 R$  and an intercept of  $\log R/Nh + \Delta S^*/2.303 R$ , from which the values of  $\Delta S^*$  and  $\Delta H^*$  were calculated and listed in Table 2. The positive signs of enthalpies ( $\Delta H^*$ ) reflect the endothermic nature of dissolution process. This suggests that mild steel dissolution requires more energy in 1 M HCl in the presence of fruit extract. The shift towards positive value of entropies( $\Delta S^*$ ) imply that the activated complex in the rate determining step represents dissociation rather than association, meaning that disordering increases on going from reactants to the activated complex [31].

**Table 2** Activation parameters  $E_a$ ,  $\Delta H^*$  and  $\Delta S^*$  for the mild steel dissolution in 1 M HCl in the absence and the presence of different fruit extracts at optimum concentrations

Inhibitor	$E_a$ (kJ mol <sup>-1</sup> )	$\Delta H^*$ (kJ mol <sup>-1</sup> )	$\Delta S^*$ (J mol <sup>-1</sup> K <sup>-1</sup> )	$\Delta G$ (kJ mol <sup>-1</sup> )
1 M HCl	28.6	22.17	-136.90	-
<i>Piper longum</i>	64.7	62.0	-36.1	-34.0
<i>Moringa oleifera</i>	119.5	116.8	140.3	-106.2
<i>Citrus aurantium</i>	54.9	52.2	-56.0	-31.8

### 3.2. EIS Measurement

The impedance spectra for Nyquist plots were analyzed by fitting to the equivalent circuit model (Fig. 3) which was used elsewhere to describe iron / acid interface [32]. In this equivalent circuit,  $R_s$  is the solution resistance,  $R_{ct}$  is the charge transfer resistance and CPE is a constant phase element. The capacitance values were calculated using the equation [33]:

$$Z_{CPE} = Q^{-1} (j\omega)^{-n} \quad (9)$$

where  $Q$  is the CPE constant,  $j$  is the imaginary unit,  $\omega$  is the angular frequency ( $\omega = 2\pi f$ , the frequency in Hz), and  $n$  is the CPE exponent which can be used as a gauge of the heterogeneity and gives details about the degree of surface inhomogeneity (roughness). Depending on the value of  $n$ , CPE can represent resistance ( $n = 0$ ,  $Q = 1/R$ ), capacitance ( $n = 1$ ,  $Q = C$ ), inductance ( $n = -1$ ,  $Q = 1/L$ ) or Warburg element ( $n = 0.5$ ).

When  $n = 1$ , this is the same equation as that for the impedance of a capacitor, where  $Q = C_{dl}$ . In fact, when  $n$  is close to 1, the CPE resembles a capacitor, but the phase angle is not 90°. It is constant and somewhat less than 90° at all frequencies.

In spite of the mentioned fact, the term, double layer capacitance, is still often used in the evaluation of AC impedance results to characterize the double layer believed to be formed at the metal/solution interface of systems displaying non-ideal capacitive behavior. For providing simple comparison between the capacitive behaviors of different corrosion systems, the values of  $Q$  were converted to  $C_{dl}$ .

$$C_{dl} = Q (\omega_{max})^{n-1} \quad (10)$$

here,  $\omega_{max}$  represents the frequency at which the imaginary component reaches a maximum. It is the frequency at the top of the depressed semicircle, and it is also the frequency at which the real part ( $Z_r$ ) is midway between the low and high frequency x-axis intercepts.

Impedance spectra for mild steel in 1 M HCl in absence and presence of optimum concentrations of fruits extract i.e. 600 ppm for *Piper longum*, 300 ppm for *Moringa oleifera* and 1200 ppm for *Citrus aurantium* are shown in the form of Nyquist plots (Fig. 4a), Bode-modulus plots (Fig. 4b) and Bode plots in the Theta-frequency format (Fig. 4c). It can be seen from Figs. 4 that diameter of the semicircular capacitive loop (Fig. 4a), and phase angle (Fig. 4c) increased with increasing concentration of fruit extract, and impedance of the double layer (Fig. 4b) decreased with extract concentration. Nyquist plots consist of a “depressed” semicircle with one capacitive loop and depressed semicircle has a centre under the real axis. Such behaviour is characteristic for solid electrodes and often referred to as frequency dispersion and has been attributed to roughness and other inhomogeneities of solid surface [34, 35]. The Nyquist plots show a depressed capacitive loop in the high frequency (HF) range. The HF capacitive loop can be attributed to the charge transfer reaction and time constant of the electric double layer and to the surface inhomogeneity of structural or interfacial origin, such as those found in adsorption processes [36]. The impedance parameters such as solution resistance ( $R_s$ ), charge transfer resistance ( $R_{ct}$ ),  $Q$ ,  $n$ , derived double layer capacitance ( $C_{dl}$ ) and inhibition efficiency ( $\eta$  %) are listed in Table 3. The values of  $\eta$ % are calculated using the following equation:

$$\eta(\%) = \frac{R_{ct,i} - R_{ct,0}}{R_{ct,i}} \times 100 \tag{11}$$

where,  $R_{ct,i}$  and  $R_{ct,0}$  are charge transfer resistances in presence and absence of inhibitor, respectively. It is clear from Table 3 that by increasing the inhibitor concentration, the  $C_{dl}$  values tend to decrease and the inhibition efficiency increases. The decrease in  $C_{dl}$  values can be attributed to a decrease in local dielectric constant and / or an increase in the thickness of the electrical double layer, suggesting that fruits extract act by adsorption at the mild steel / solution interface [37]. On the other hand, the values of  $C_{dl}$  decreased with an increase in the extract concentration. This situation was the result of an increase in the surface coverage by the inhibitor, which led to an increase in the inhibition efficiency. The values of the phase shift indicate that the  $C_{dl}$  values are in reasonable confidence limit. Also any significant change in the values of the phase shift,  $n$ , was not observed in the absence and in the presence of fruits extract. To predict the dissolution mechanism, the value of  $n$  can be used as an indicator [38]. The values of  $n$ , ranging between 0.827 and 0.869, indicate that the charge transfer process controls the dissolution mechanism of mild steel in 1 M HCl solution in the absence and in the presence of fruit extract. The thickness of the protective layer,  $\delta_{org}$ , was related to  $C_{dl}$  by the following equation [39].

$$\delta_{org} = \frac{\epsilon_0 \epsilon_r}{C_{dl}} \tag{12}$$

where,  $\epsilon_0$  is the dielectric constant and  $\epsilon_r$  is the relative dielectric constant. This decrease in the  $C_{dl}$ , which can result from a decrease in local dielectric constant and/or an increase in the thickness of the electrical double layer, suggested that fruits extract function by adsorption at the metal/solution interface. Thus, the change in  $C_{dl}$  values was caused by the gradual replacement of water molecules by the adsorption of the organic molecules on the metal surface, decreasing the extent of metal dissolution [40].

**Table 3** Electrochemical impedance parameters for mild steel in 1 M HCl in the absence and presence different fruits extract at their optimum concentrations

Name of inhibitor	Inhibitor concentration	$R_{ct}$ ( $\Omega \text{ cm}^2$ )	$Q$ ( $\mu\text{F cm}^2$ )	$n$	$C_{dl}$ ( $\mu\text{F cm}^2$ )	$\eta$ (%)
1 M HCl	-	8.5	250.0	0.827	68.9	-
<i>Piper longum</i>	240.0	213.2.1	84.8	0.869	46.4	96.0
	300.0	273.3	73.9	0.855	33.1	96.9
	600.0	355.5	54.8	0.849	27.3	97.6
<i>Moringa oleifera</i>	200.0	215.0	91.3	0.829	43.0	96.0
	250.0	324.5	77.9	0.829	41.4	97.3
	300.0	644.9	61.7	0.854	32.4	98.6
<i>Citrus aurantium</i>	300.0	23.5	151.7	0.866	68.5	68.9
	600.0	58.2	148.9	0.861	65.4	85.4
	1200.0	65.2	123.0	0.854	56.3	87.0

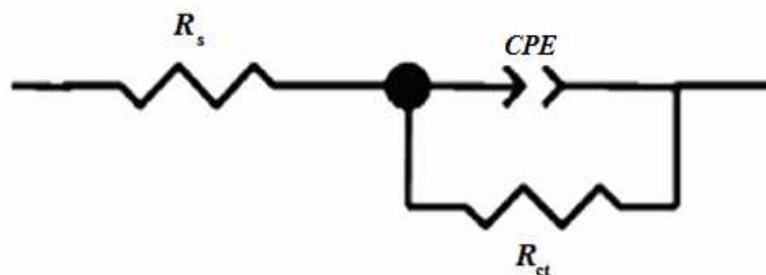


**Fig. 3.** Electrochemical equivalent circuit used to fit the impedance spectra

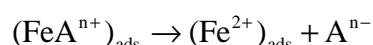
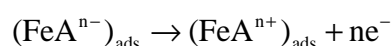
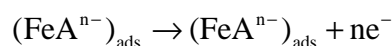
It is apparent from Nyquist plots that the impedance response of mild steel in inhibited HCl solution has significantly changed after the addition of fruits extract in acid solution and that the impedance of inhibited substrate increases with increasing conc. of inhibitor. The Nyquist plots showed that on increasing extract concentration, charge transfer resistance increases and double layer capacitance decreases. From the Table 3, it is clear that the greatest effect was observed at 300 ppm of (*Moringa oleifera*) extract which gives  $R_{ct}$  value of 644.9  $\Omega\text{cm}^2$  in 1 M HCl respectively. Inhibition efficiency is found to increase with inhibitor concentration in the acid.

**3.3. Polarization Measurements**

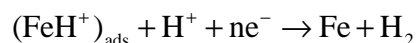
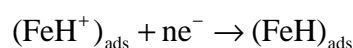
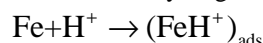
Polarization curves for mild steel at optimum concentration of fruits extract in aerated solutions are shown in Fig. 4d. The extrapolation of Tafel straight line allows the calculation of the corrosion current density ( $I_{corr}$ ). The values of  $I_{corr}$ , the corrosion potential ( $E_{corr}$ ), cathodic and anodic Tafel slopes ( $b_c$ ,  $b_a$ ) and inhibition efficiency ( $\eta$  %) are given in Table 4. The values of  $I_{corr}$  were found to decrease in the presence of inhibitors. The decrease in  $I_{corr}$  values can be due to the adsorption of fruits extract on the mild steel surface. It was observed that there is a small shift towards cathodic region in the values of  $E_{corr}$ . In present study, maximum displacement in  $E_{corr}$  value was 69 mV, which indicates that all studied fruits extract were mixed-type inhibitors. The ( $\eta$  %) is calculated using the following equation:

$$\eta\% = \left( \frac{I_{corr}^0 - I_{corr}^i}{I_{corr}^0} \right) \times 100 \tag{13}$$

where,  $I_{corr}^0$  and  $I_{corr}^i$  are the corrosion current density values without and with inhibitor, respectively. Some of the authors proposed the following mechanism for the corrosion of iron and steel in acid solution [41-43]:



The cathodic hydrogen evolution



The change in  $b_a$  and  $b_c$  values as shown in Table 4 indicates that adsorption of fruits extract modify the mechanism of anodic dissolution as well as cathodic hydrogen evolution. From the Fig. 4d, it is clear that both the cathodic and anodic reactions are inhibited and the inhibition increases as the inhibitor conc. increases in acid media, but the cathode is more polarized. Linear polarization values are shown in Table 5.

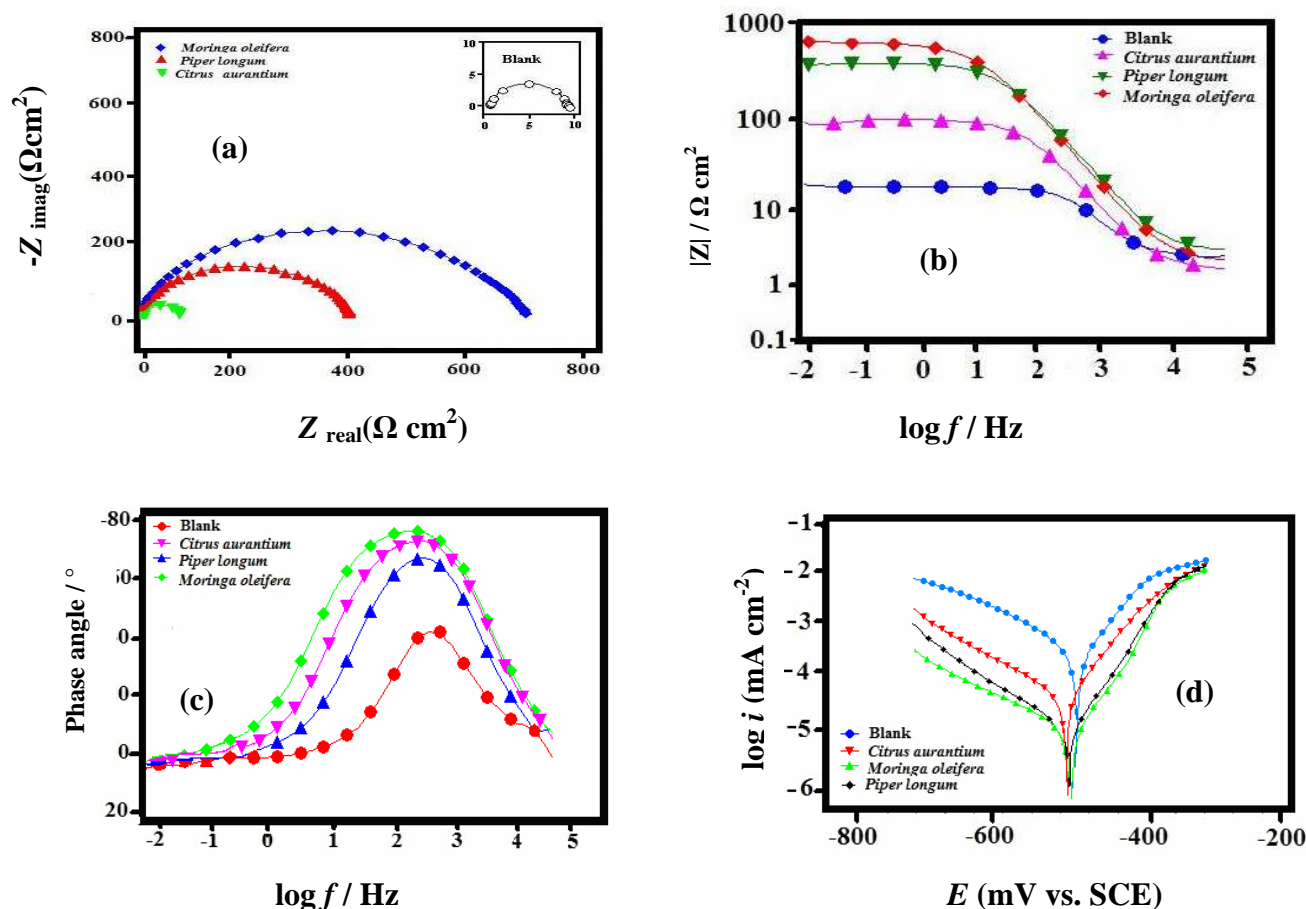


**Fig. 4**(a) Nyquist plots, (b) Bode-modulus plots, and (c) Bode-phase angle plots (d) Tafel plots in absence and presence of different concentrations of extract in 1 M HCl.

**Table 4** Tafel Polarization parameters for mild steel in 1 M HCl in the absence and presence of different fruits extract at their optimum concentrations

Name of Inhibitor	Inhibitor concentration (ppm)	$-E_{corr}$ (mV vs SCE)	$b_a$ (mV / dec)	$b_c$ (mV / dec)	$i_{corr}$ (mA / cm <sup>2</sup> )	$\eta$ (%)
1 M HCl	-	446	90.4	121.0	1540.0	-
<i>Piper longum</i>	240.0	464	66.0	116.0	53.0	96.5
	300.0	469	78.0	138.0	46.0	96.9
	600.0	479	72.0	124.0	41.0	97.3
<i>Moringa oleifera</i>	200.0	503	51.0	58.0	59.0	96.1
	250.0	472	48.0	54.0	38.0	97.5
	300.0	493	36.0	34.0	28.0	98.1
<i>Citrus aurantium</i>	300.0	466	71.0	263.0	430.0	72.0
	600.0	515	121.0	128.0	212.0	86.2
	1200.0	464	71.0	114.0	160.0	89.6

**Table 5** Linear Polarization parameters for mild steel in 1 M HCl in the absence and presence of different fruits extract at their optimum concentrations

Name of Inhibitor	Inhibitor concentration (ppm)	$R_p$ ( $\Omega$ cm <sup>2</sup> )	$\eta$ (%)
1 M HCl	-	9.7	-
<i>Piper longum</i>	240	270.6	96.4
	300	351.0	97.2
	600	391.1	97.5
<i>Moringa oleifera</i>	200	252.7	96.1
	250	342.0	97.1
	300	564.2	98.2
<i>Citrus aurantium</i>	300	33.8	71.3
	600	85.6	88.6
	1200	92.0	89.4

3.4. Adsorption Isotherm and free energy of adsorption

The adsorption of an organic adsorbate on to metal-solution interface can be represented by a substitutional adsorption process between the organic molecules in the aqueous solution phase ( $Org_{(sol)}$ ) and the water molecules on the metallic surface ( $H_2O_{(ads)}$ ) [44].



where,  $x$  is the size ratio representing the number of water molecules replaced by one molecule of organic adsorbate. Basic information on the interaction between the inhibitor and the mild steel surface can be provided by the adsorption isotherm. For this purpose, the values of surface coverage ( $\theta$ ) at different concentrations ( $C_{inh}$ ) of fruits extract in acid media in the temperature range (308-338 K) have been used to explain the best isotherm to determine the adsorption process. The values of  $\theta$  can be easily determined from the ratio ( $\eta$  %)/100, where ( $\eta$  %) was obtained from weight loss measurements. Attempts were made to fit these  $\theta$  values to various isotherm including Frumkin, Langmuir, Temkin. According to these isotherms,  $\theta$  is related to the inhibitor concentration,  $C_{inh}$ :

$$\theta = \frac{bC_{inh}}{1+bC_{inh}} \tag{Langmuir isotherm} \tag{15}$$

$$\exp(-2a\theta) = K_{ads} C_{inh} \tag{Temkin isotherm} \tag{16}$$

where,  $b$  designates the adsorption coefficient in equation (15),  $a$  the molecular interaction parameter,  $K_{ads}$  is the equilibrium constant of the adsorption process in equation (16). The best fit was obtained with Langmuir isotherm as

shown in Fig. 5. The value of regression coefficients ( $R^2 = 0.999$ ) in *Moringa oleifera* (0.990) in *Citrus Aurantium* and (0.999) in *Piper longum* confirms the validity of this approach.

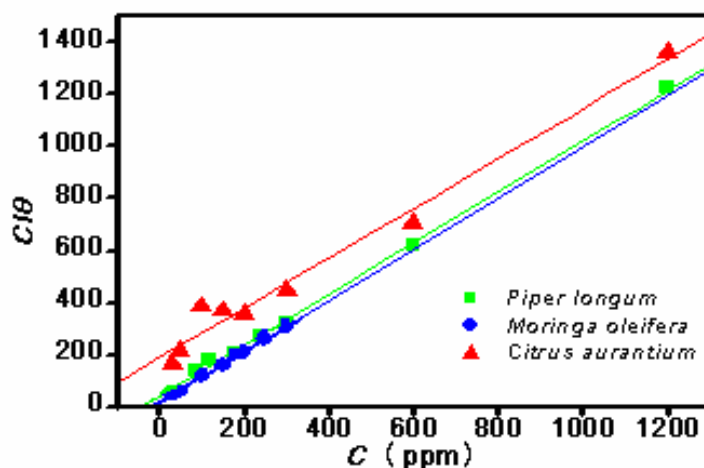


**Fig. 5.** Langmuir adsorption isotherm plot for the adsorption of extract in 1 M HCl on the surface of mild steel.

### 3.5. Fourier transform infrared spectroscopy (FTIR) analysis

It has been established that FTIR spectrophotometer is a powerful instrument that can be used to determine the type of bonding for organic inhibitors adsorbed on the metal surface. In present study, reflectance FTIR spectra were used to support the fact that corrosion inhibition of mild steel in acid media is due to the adsorption of inhibitor molecules on the mild steel surface. The prominent peaks are given in Table 6. From data in Table 6, it can be established that inhibition of corrosion of mild steel in 1 M HCl solution by fruits extract was due to the adsorption of extract's constituents on the mild steel surface.

**Table 6** IR spectral data (significant peaks  $\nu_{\max}$  in  $\text{cm}^{-1}$  (KBr))

3268 $\text{cm}^{-1}$	(N–H, O–H str)
2883 $\text{cm}^{-1}$	(O–H, (COOH) str)
1725 $\text{cm}^{-1}$	(C=O str)
1528 $\text{cm}^{-1}$	(C=N str)
1082 $\text{cm}^{-1}$	(C–O str) for <i>Moringa oleifera</i> .
3889 $\text{cm}^{-1}$	(Fe–O bending)
3621 $\text{cm}^{-1}$	(O–H, str)
3338 $\text{cm}^{-1}$	(N–H str)
3154 $\text{cm}^{-1}$	(C–H str)
2744 $\text{cm}^{-1}$	(O–H, (COOH) str)
1642 $\text{cm}^{-1}$	(C=O str)
1184 $\text{cm}^{-1}$ , 1087 $\text{cm}^{-1}$	(C–O str), for <i>Citrus aurantium</i> .
3298 $\text{cm}^{-1}$	(O–H str)
2884 $\text{cm}^{-1}$	(C–H str)
1725 $\text{cm}^{-1}$	(C=O str)
1534 $\text{cm}^{-1}$ , 1450 $\text{cm}^{-1}$	(C=C (Ar) str)
1373 $\text{cm}^{-1}$	(C–H bending)
1082 $\text{cm}^{-1}$	(C–O str) for <i>Piper longum</i> .

## 4. Mechanism of inhibition

The transition of metal/solution interface from a state of active dissolution to the passive state is attributed to the adsorption of the inhibitor molecules at the metal/solution interface, forming a protective film. The rate of adsorption is usually rapid and hence, the reactive metal surface is shielded from the aggressive environment [45].

Adsorption process can occur through the replacement of solvent molecules from metal surface by ions and molecules accumulated in the vicinity of metal/solution interface. Ions can accumulate at the metal/solution interface in excess of those required to balance the charge on the metal at the operating potential. These ions replace solvent molecules from

the metal surface and their centers reside at the inner Helmholtz plane. This phenomenon is termed specific adsorption, contact adsorption. The anions are adsorbed when the metal surface has an excess positive charge in an amount greater than that required to balance the charge corresponding to the applied potential. Aromatic compounds (which contain the benzene ring) undergo particularly strong adsorption on many electrode surfaces. The bonding can occur between metal surface atoms and the aromatic ring of the adsorbate molecules or ligands substituent groups. The exact nature of the interactions between a metal surface and an aromatic molecule depends on the relative coordinating strength towards the given metal of the particular groups present [46].

The main constituents of the fruits extracts are Arginine (*Moringa oleifera*), Piperine, Piplartine, Rutin (*Piper longum*) and Threonine (*Citrus Aurantium*) whose structures are given in Fig. 6. The inhibition efficiency afforded by fruits extracts may be attributed to the presence of N, O atoms,  $\pi$ -electrons and/or aromatic/heterocyclic rings. Experimentally determined values of  $\eta\%$  for three fruits extract studied are in the order *Moringa oleifera* > *Piper longum* > *Citrus aurantium*. This order of inhibition efficiency can be best explained in terms of their structures. The highest inhibition efficiency shown by *Moringa oleifera* fruit extract can be attributed to the presence of imine (C=N) group, four N atoms and long alkyl chain. The relatively weaker inhibition performance of *Citrus aurantium* is due to the presence of electron withdrawing COOH group, which decreases the electron density on nitrogen atom.

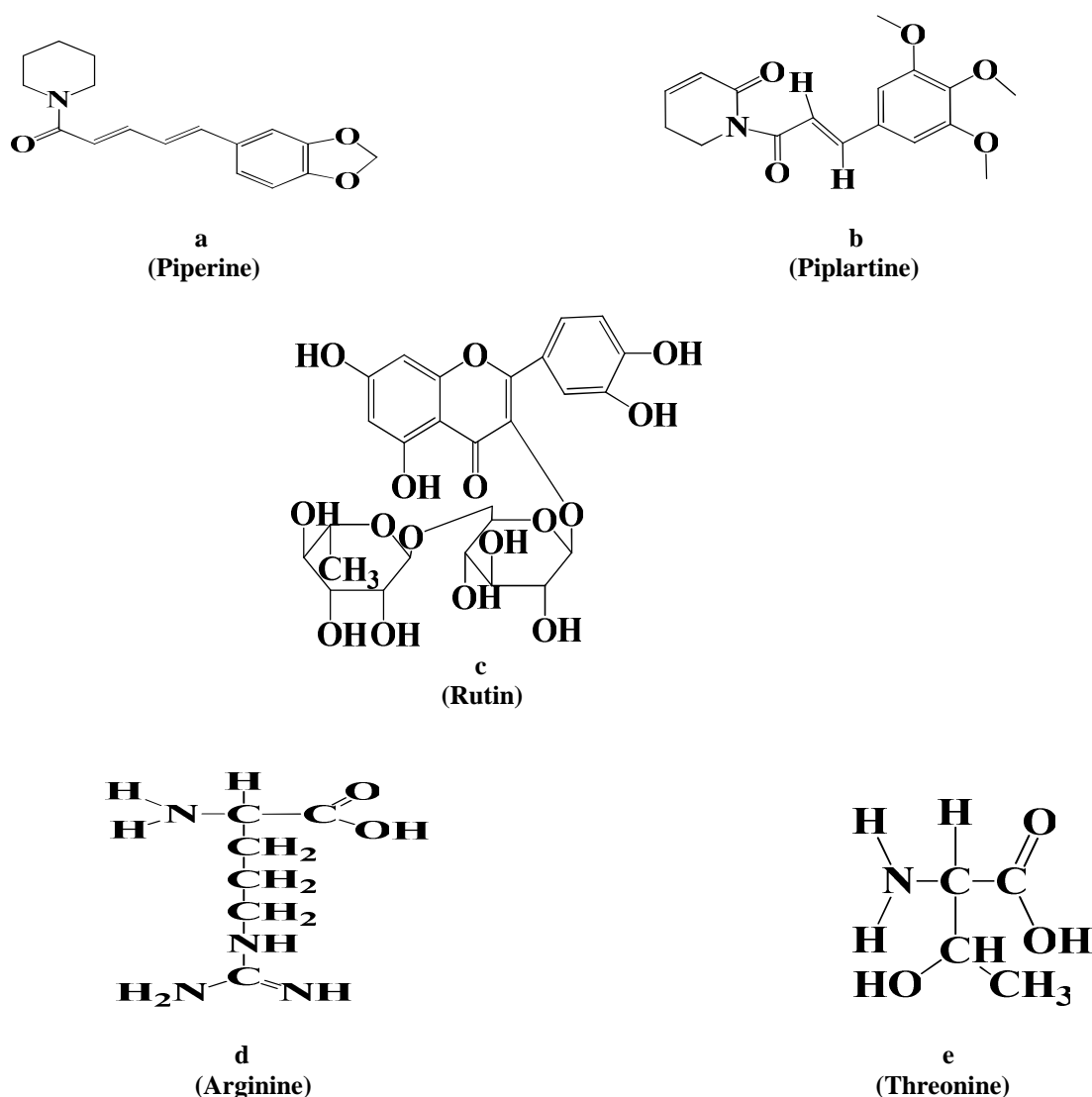


Fig. 6. Structure of main constituents of fruits extract

It is not possible to consider a single adsorption mode between inhibitor and metal surface because of the complex nature of adsorption and inhibition of a given inhibitor. The adsorption of main constituents of fruit extract can be attributed to the presence of O-atoms,  $\pi$ -electrons and aromatic/heterocyclic rings. Presence of methoxy group also enhances the inhibition efficiency. Therefore, the possible reaction centres are unshared electron pair of hetero-atoms and  $\pi$ -electrons of aromatic/heterocyclic ring. In aqueous acidic solutions, main constituents exist either as neutral molecules or as protonated molecules (cations). The inhibitors may adsorb on the metal/acid solution interface by one and/or more of the following ways: (i) electrostatic interaction of protonated molecules with already adsorbed

chloride ions, (ii) donor-acceptor interactions between the  $\pi$ -electrons of aromatic ring and vacant d orbital of surface iron atoms, (iii) interaction between unshared electron pairs of hetero atoms and vacant d-orbital of iron surface atoms.

Generally two modes of adsorption are considered on the metal surface in acid media. In one mode, the neutral molecules may be adsorbed on the surface of mild steel through the chemisorption mechanism, involving the displacement of water molecules from the mild steel surface and the sharing electrons between the hetero atoms and iron. The inhibitor molecules can also adsorb on the mild steel surface on the basis of donor-acceptor interactions between  $\pi$ -electrons of the aromatic / heterocyclic ring and vacant d-orbitals of surface iron atoms. In second mode, since it is well known that the steel surface bears positive charge in acid solution [52], so it is difficult for the protonated molecules to approach the positively charged mild steel surface ( $\text{H}_3\text{O}^+$ /metal interface) due to the electrostatic repulsion. Since chloride ions have a smaller degree of hydration, thus they could bring excess negative charges in the vicinity of the interface and favour more adsorption of the positively charged inhibitor molecules, the protonated inhibitors adsorb through electrostatic interactions between the positively charged molecules and the negatively charged metal surface. Thus there is a synergism between adsorbed  $\text{Cl}^-$  ions and protonated inhibitors. Thus inhibition of mild steel corrosion in 1 M HCl is due to the adsorption of extract constituents on the mild steel surface. This assumption could be further confirmed by the reflectance FTIR analysis of mild steel surface.

## 5. Conclusion

1. Fruits extract are good inhibitor for mild steel corrosion in 1 M HCl solution. Inhibition efficiency increases with increasing fruits extract concentration and  $\eta\%$  values obtained from different methods employed are in reasonable agreement.
2. The adsorption of fruits extract on mild steel surface obeyed Langmuir adsorption isotherm. Adsorption is neither typical physisorption nor typical chemisorption but it is complex in nature.
3. Polarization curves measurements indicate that fruits extract acted as mixed type inhibitor.
4. The reflectance FTIR analysis showed that the inhibition of mild steel corrosion occurred due to the formation of a protective film on the metal surface through adsorption of constituents of fruits extract.

## References

1. Ashassi-Sorkhabi, H., Seifzade, D., Hosseini, M.G. *Corros. Sci.* 50 (2008) 3363.
2. Satapathy, A.K., Gunasekaran, G., Sahoo, S.C., Kumar, A., Rodrigues, P.V. *Corros. Sci.* 51 (2009) 2848.
3. Abdel-Gaber, A.M., Abd-El-Nabey, B.A., Saadawy, M. *Corros. Sci.* 51 (2009) 1038-1042.
4. Raja, P.B., Sethuraman, M.G. *Mater. Lett.* 62 (2008) 113.
5. Noor, E.A. *J. Engg. Appl. Sci.* 3 (2008) 23.
6. Buchweishaija, J., Mhinzi, G.S. *Port. Electrochim. Acta* 26 (2008) 257.
7. Oguzie, E.E. *Corros. Sci.* 50 (2008) 2993.
8. Okafor, P.C., Ikpi, M.E., Uwaha, I.E., Ebenso, E.E., Ekpe, U.J., Umoren, S.A. *Corros. Sci.* 50 (2008) 2310.
9. Valek, L., Martinez, S. *Mater. Lett.* 61 (2007) 148.
10. Oguzie, E.E. *Corros. Sci.* 50 (2008) 2993.
11. Singh, Ambrish, Ahamad, I., Singh, Vinod Kumar, Quraishi, M.A. (2010) *J.S.E.L.* 2010 JSEL-D-10-00143R2.
12. Noor, E.A. *J. Appl. Electrochem.* 39 (2009) 1465.
13. De Souza, F.S., Spinelli, A. *Corros. Sci.* 51 (2009) 642.
14. Raja, P.B., Sethuraman, M.G. *Mater. Lett.* 62 (2008) 1602.
15. El-Etre, A.Y. *Corros. Sci.* 45 (2003) 2485.
16. Badiea, A.M., Mohana, K.N. *J. Mater. Eng. Perform.* 18 (2009) 1264.
17. Chauhan, L.R., Gunasekaran, G. *Corros. Sci.* 49 (2007) 1143.
18. El-Etre, A.Y., Abdallah, M., El-Tantawy, Z.E. *Corros. Sci.* 47 (2005) 385.
19. Orubite, K.O., Oforka, N.C. *Mater. Lett.* 58 (2004) 1768.
20. Evc Grassino, A.N., Grabaric, Z., Pezzani, A., Fasanaro, G., Voi, A.L. *Food Chem. Toxicol* 47 (2009) 1556.
21. Torres-Acosta, A.A. *J. Appl. Electrochem.* 37 (2007) 835.
22. Quraishi, M.A., Singh, Ambrish, Singh, Vinod Kumar, Yadav, Dileep Kumar, Singh, Ashish Kumar *Mater. Chem. Phy.* 122 (2010) 114.
23. Quraishi, M.A., Yadav, Dileep Kumar, Ahamad Ishtiaque *The Open Corrosion Journal* 2 (2009) 56.
24. Schorr, M., Yahalom, J. *Corros. Sci.* 12 (1972) 867.
25. Quraishi, M.A., Khan, S. *Ind. J. Chem. Technol.* 12 (2005) 576.
26. Breslin, C.B., Carrol, W.M. *Corros. Sci.* 34 (1993) 327.
27. Khedr, M.G.A., Lashien, M.S. *Corros. Sci.* 33 (1992) 137.
28. Larabi, L., Benali, O., Harek, Y. *Mater. Lett.* 61 (2007) 3287.
29. Szauer, T., Brandt, A. *Electrochim. Acta.* 26 (1981) 1253.

30. Bockris, J.O.M., Reddy, A.K.N. *Modern Electrochemistry* Plenum Press, New York (1977).
31. Prabhu, R.A., Shanbhag, A.V., Venkatesha, T.V. *J. Appl. Electrochem.* 37 (2007) 491.
32. Mansfeld, F. *Corrosion* 36 (1981) 301.
33. Shukla, J. Pitre, K.S. *Corros. Rev.* 20 (2002) 217.
34. Elayyachy, M., Idrissi, A., Hammouti, B. *Corros. Sci.* 48 (2006) 2470.
35. Martinez, S., Metikos-Hukovic, M. *J. Appl. Electrochem.* 33 (2003) 1137.
36. Goncalves, R.S., Azambuja, D.S., Serpa Lucho, A.M. *Corros. Sci.* 44 (2002) 467.
37. Yurt, A., Bereket, G., Kivrak, A., Balaban, A., Erk, B. *J. Appl. Electrochem.* 35 (2005) 1025.
38. Hermas, A.A., Morad, M.S., Wahdan, M.H. *J. Appl. Electrochem.* 34 (2004) 95.
39. Bentiss, F., Mehdi, B., Mernari, B., Traisnel, M., Vezin, H. *Corrosion* 58 (2002) 399.
40. Anand, R.R., Hurd, R.M., Hackerman, N. *J. Electrochem. Soc.* 112 (1965) 138.
41. Morad, M.S., El-Dean, A.M.K. *Corros. Sci.* 48 (2006) 3398.
42. Tebbji, K., Hammouti, B., Oudda, H., Ramdani, A., Benkaddour, M. *Appl. Surf. Sci.* 252 (2005) 1378.
43. Yurt, A., Balaban, A., Ustun Kandemir, S., Bereket, G., Erk, B. *Mater. Chem. Phy.* 85 (2004) 420.
44. Chao, C.Y., Lin, L.F., Macdonald, D.D. *J. Electrochem. Soc.* 128 (1981) 1187.
45. Ritchie, I.M., Bailey, S., Woods, R. *Adv. Colloid. Interface. Sci.* 80 (1999) 183.
46. Trabellini, G., Mansfeld, F. *Corrosion Mechanisms* Marcel Dekker New York (1987) 109.

(2010) [www.jmaterenvironsci.com](http://www.jmaterenvironsci.com)